DOI: 10.1111/nyas.14906

CONCISE REPORT

ANNALS OF THE NEW YORK ACADEMY OF SCIENCES

Electrical conductivity through π–π stacking in a two-dimensional porous gallium catecholate metal–organic framework

Grigorii Skorupskii[1,#,†] | **Géraldine Chanteux**[2,#] | **Khoa N. Le**[3] | **Ivo Stassen**[1] | **Christopher H. Hendon**[3] | **Mircea Dincă**[1]

[1]Department of Chemistry, Massachusetts Institute of Technology, Cambridge, Massachusetts, USA

[2]Institute of Condensed Matter and Nanosciences, Université catholique de Louvain, Ottignies-Louvain-la-Neuve, Belgium

[3]Department of Chemistry and Biochemistry, University of Oregon, Eugene, Oregon, USA

Correspondence
Mircea Dincă, Department of Chemistry, Massachusetts Institute of Technology, 77 Massachusetts Ave., Cambridge, MA 02139, USA.
Email: mdinca@mit.edu

[#]Grigorii Skorupskii and Géraldine Chanteux contributed equally.
[†]Present address: Grigorii Skorupskii, Department of Chemistry, Princeton University, Princeton, New Jersey, USA.

Funding information
National Science Foundation, Grant/Award Numbers: DMR-2105495, DMR-1956403; Research Corporation for Science Advances

Abstract

Metal–organic frameworks (MOFs) are hybrid materials known for their nanoscale pores, which give them high surface areas but generally lead to poor electrical conductivity. Recently, MOFs with high electrical conductivity were established as promising materials for a variety of applications in energy storage and catalysis. Many recent reports investigating the fundamentals of charge transport in these materials focus on the role of the organic ligands. Less consideration, however, is given to the metal ion forming the MOF, which is almost exclusively a late first-row transition metal. Here, we report a moderately conductive porous MOF based on trivalent gallium and 2,3,6,7,10,11-hexahydroxytriphenylene. Gallium, a metal that has not been featured in electrically conductive MOFs so far, has a closed-shell electronic configuration and is present in its trivalent state—in contrast to most conductive MOFs, which are formed by open-shell, divalent transition metals. Our material, made without using any harmful solvents, displays conductivities on the level of 3 mS/cm and a surface area of 196 m^2/g, comparable to transition metal analogs.

KEYWORDS
electrical transport, metal-organic frameworks, porous conductors, semiconductor materials

INTRODUCTION

The past decade saw an explosion of interest in electrically conductive metal–organic frameworks (MOFs).[1] These materials, constructed from metal ions and organic linkers, feature high surface areas and porosity. This combination of conductivity and porosity is often their main attraction—allowing applications such as supercapacitor electrode materials,[2] oxygen reduction catalysts,[3] and chemiresistive sensors.[4,5] Another advantage of conductive MOFs lies in their intrinsic tunability owing to both the combinatorial diversity of accessible structural building blocks, as well as the possibility of functionalizing the organic fragments. Despite the extensive research into these materials, the mechanisms of charge transport within them—and the origin of the high conductivities—are not yet fully understood.[1]

The highest electrical conductivities are seen in two-dimensional (2D) MOFs, which are homologous to Ni_3(2,3,6,7,10,11-hexaiminotriphenylene)$_2$[6] and hold the record for room-temperature electrical conductivity in MOFs and other porous solids (150 S/cm for single crystals).[7] Studies of 2D conductive MOFs have largely focused on identifying the role of the organic linkers. Extensive research has

been devoted to evaluating the importance of metal-linker covalency by varying the linkers and their functional groups.[1] Comparatively less focus has been given to the metal used, and the list of metal ions used in 2D conductive MOFs is generally limited to late first-row divalent transition metal ions, such as Ni(II), Co(II), and Cu(II).[5,6,8–10]

Here, we expand the list of metals used in 2D conductive MOFs to include gallium in order to analyze the effects of the higher cationic charge of Ga(III)—and its closed-shell configuration—on 2D conductive MOF's electrical transport properties. We paired the oxophilic Ga(III) with the oxygen-based 2,3,6,7,10,11-hexahydroxytriphenylene (H_6HOTP) ligand to form a layered electrically conductive porous MOF. The material is synthesized in mild conditions without the use of any organic solvents, making the material suitable for environmentally conscious applications. The electrical conductivity of the material was above 3 mS/cm, which is similar[3] to previously reported[11] Ni(II) and Co(II)-based homologous MOFs. Based on *ab initio* electronic structure calculations, we believe π–π stacking interactions provide a pathway for electronic transport in the material, and this accounts for the similarity in electrical conductivity to the Ni(II) and Co(II) analogs despite the different chemistry of the metal nodes.

RESULTS AND DISCUSSION

The reaction of gallium(III) sulfate, gallium(III) nitrate, and 2,3,6,7,10,11-hexahydroxytriphenylene (H_6HOTP) in deionized water at 80°C afforded a dark teal microcrystalline powder with the overall formula (excluding noncoordinated solvent) of $Ga_9(H_2O)_{30}(HOTP)_4(SO_4)_6$ (**Ga_9(HOTP)$_4$**). Importantly, this synthesis uses no toxic or environmentally harmful organic solvents or transition metals. Synthesis was performed at relatively low temperatures, making this material a considerably "greener" alternative to most other conductive MOFs, which often require the use of dimethylformamide (or similar solvents)[11] or employ toxic and carcinogenic metals, such as nickel.[6] Although the material's formula demands only the presence of sulfate anions, we found that controlling the solution's pH level via the addition of nitrate salt into the reaction mixture significantly improved the material's crystallinity. The resulting powder consisted of nanoscale hexagonal needles (Figure 1E), which were, due to their small size, unsuitable for single-crystal X-ray diffraction. The powder did, however, produce bright and well-resolved powder X-ray diffraction (PXRD) patterns, which strongly resembled those of the previously reported[11] Co(II) and Ni(II)-based materials. In order to improve our understanding of the structure of **Ga_9(HOTP)$_4$**, we took advantage of this similarity and performed a Rietveld refinement[12] (Figure 2) of the PXRD data for **Ga_9(HOTP)$_4$** using the reported model for **Co_9(HOTP)$_4$** as a starting point. The resulting structure is shown in Figure 1. Detailed synthetic and characterization methods are provided in the Supplementary Material.

Ga_9(HOTP)$_4$ crystallizes in the trigonal space group $P\bar{3}c1$ with a = 21.6972(12) Å and c = 13.7911(11) Å. The structure consists of interleaved layers of $[(H_2O)_4Ga]_3$(HOTP) molecular clusters (Figure 1B), and polymeric layers of the overall formula $[(H_2O)_2Ga]_3(HOTP)_2$ (Figure 1C). These layers are separated by approximately 3.45 Å, which is a fairly typical[13] distance for π–π stacked aromatic carbon moieties. Compared to the reported structure[11] of $Co_9(HOTP)_4$, this structure has two critical dissimilarities. First, the structure incorporates ordered sulfate anions, seemingly to compensate for the higher cationic charge of Ga(III). This leads to a significant reduction in the accessible pore volume, with the pore diameter decreasing to ~8 Å. Second, whereas the Co and Ni-based materials show significant buckling within the polymeric layers, here, the layers lay flat. The layer stacking distance for **Ga_9(HOTP)$_4$** is also larger than in its transition metal analogs (~3.45 vs. ~3.3 Å for **Co_9(HOTP)$_4$**), and the two features may share a common origin. One possibility may lie in hydrogen bonding interactions between the apically coordinated water molecules and the linkers' oxygen atoms—these interactions perhaps "squeeze" the MOF into a buckled configuration at shorter interlayer spacings, and "stretch" it into a flat layer with larger interlayer distances.

Although **Ga_9(HOTP)$_4$** has a reduced pore size and higher density compared to its Co(II) analog, it still shows a considerable Brunauer–Emmett–Teller (BET)[14] surface area of 196 m^2/g as determined from N_2 adsorption measurements (Figure 3) for material activated using supercritical CO_2 drying. The material shows a clear type-I adsorption isotherm, indicating that the observed surface area is from internal pores and not the powder's external surface. The experimental BET surface area matches well with the predicted surface area of 170 m^2/g, which was estimated from geometry-based calculations as implemented in zeo++.[15]

Ga_9(HOTP)$_4$ is moderately electrically conductive. Two-probe pressed pellet resistivity measurements over three independent batches show a median conductivity of 3 mS/cm at room temperature (Figure 4A). Intriguingly, this value is similar to those reported for **Ni_9(HOTP)$_4$** and **Co_9(HOTP)$_4$** using the same measurement setup.[3] This finding is surprising given the significant differences in the metal linkages within the polymeric layers; Ni(II) and Co(II) are divalent and have open-shell electronic configurations that contrast with trivalent, closed-shell Ga(III). We propose two potential explanations for this. First, it is possible that the measured conductivity of these materials is dominated by grain boundary resistance; powders of **Ga_9(HOTP)$_4$** have a similar crystallite morphology and size to those of its transition-metal analogs (cf. Figure 1A in Ref. 10 with Figure 1E of this work). Indeed, the temperature dependence of the electrical conductivity of **Ga_9(HOTP)$_4$** is consistent with this explanation. Pellets of **Ga_9(HOTP)$_4$** show thermally activated transport, which is fit best using a three-dimensional Mott variable-range hopping (VRH)[16] law between 100 and 290 K. Although multiple possibilities exist that could explain such a temperature dependence, it is reasonable to expect it originates in charges hopping between grains of a nanocrystalline powder. Second, the similarities in the electrical conductivities of **Ga_9(HOTP)$_4$** with its Ni(II) and Co(II) analogs may lie in the extensive π–π stacking interactions between the conjugated linkers, as we observed previously in HOTP materials with rare-earth metals.[13] Indeed, if the primary path for electrical transport is parallel to the π–π stacked columns, and not within the polymeric layers, then it is reasonable to expect little variance in electrical conductivity with a metal ion.

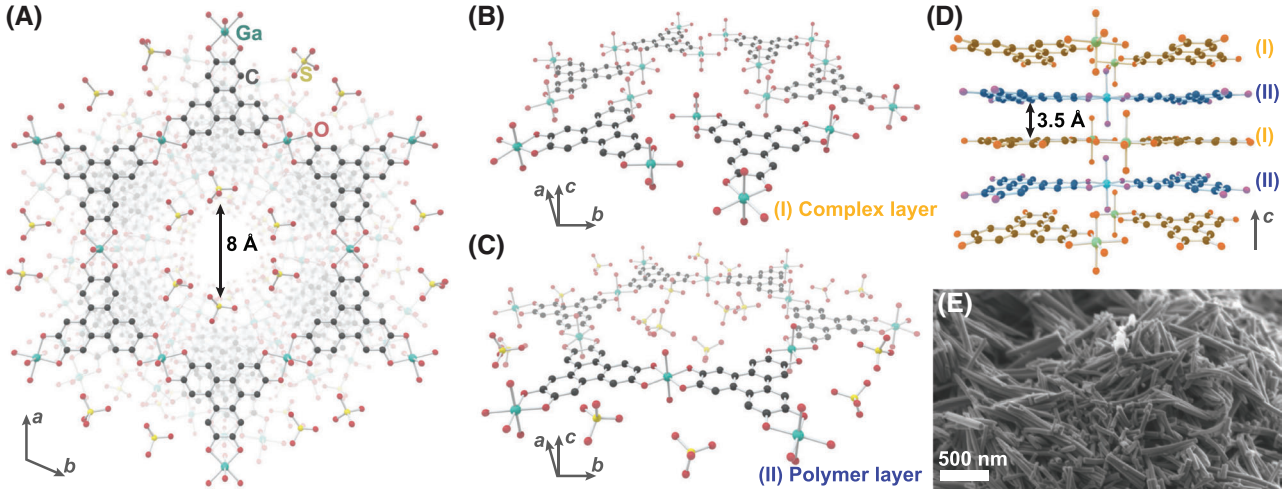

FIGURE 1 Crystal structure of **Ga_9(HOTP)$_4$**. (A) The material forms an intrinsically porous layered MOF with a pore diameter of approximately 8 Å. (B) The structure is composed of interleaved layers of molecular trinuclear complexes and (C) extended polymeric layers. (D) The layers are separated by approximately 3.5 Å, which is a typical π–π stacking distance. Unlike in the transition-metal analogs $Co_9(HOTP)_4$ and $Ni_9(HOTP)_4$, in **Ga_9(HOTP)$_4$**, we see ordered sulfate anions in the pore seemingly to compensate for the higher ionic charge of Ga. (E) Scanning electron micrograph of the microcrystalline powder illustrating the hexagonal shape of the needle-like crystallites. Hydrogen atoms and noncoordinated solvent molecules are omitted from (A–D).

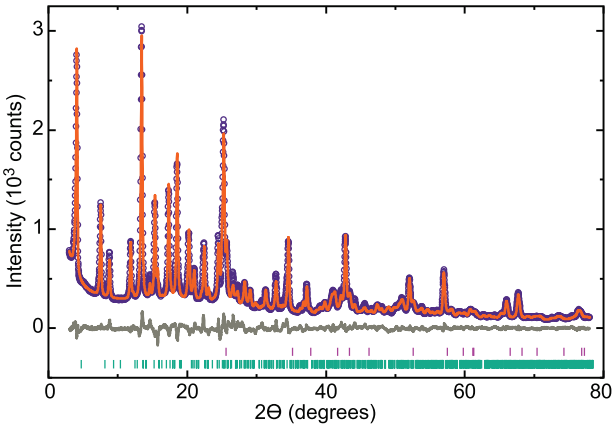

FIGURE 2 Rietveld refinement of **Ga_9(HOTP)$_4$**. The diffraction data (circles) are fitted (orange solid line) to satisfactory residuals of $R_{Bragg} = 3.10\%$, $R_{wp} = 6.83\%$, and GOF = 3.85. Gray line depicts the difference, green bars the positions of expected reflections, and purple bars reflections belonging to the internal standard Al_2O_3.

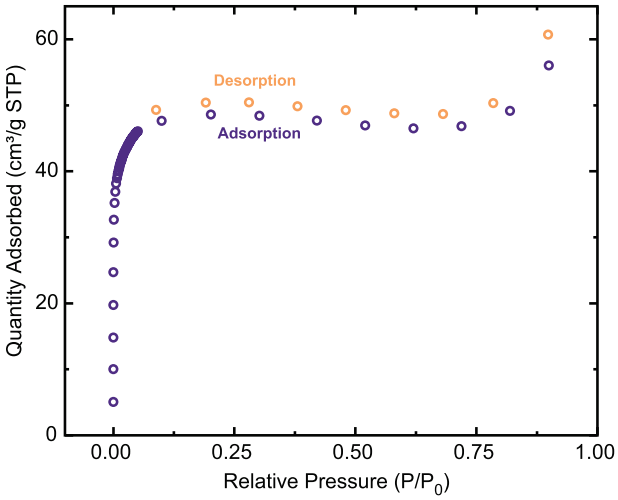

FIGURE 3 N_2 adsorption and desorption isotherms of **Ga_9(HOTP)$_4$**. The isotherms show clear type-I behavior, indicating intrinsic porosity and a BET surface area of 196 m^2/g, which matches well with the expected value for the crystal structure (170 m^2/g).

To gain better insight into the nature of charge transport in both **Ga_9(HOTP)$_4$**, we performed *ab initio* density functional theory (DFT) calculations of the electronic band structure of the material. As shown in Figure 5, **Ga_9(HOTP)$_4$** is calculated to be a narrow-gap semiconductor with a predicted band gap of 0.38 eV. The experimental optical band gap for **Ga_9(HOTP)$_4$**, as determined from diffuse reflectance measurements, was 0.36 eV, which agrees perfectly with computational predictions. Two crucial features can be seen in the band structure of **Ga_9(HOTP)$_4$**: (1) the bands along the Γ-K-M directions, which correspond to interactions within the 2D layers, are relatively flat and indicate little charge delocalization within the layers; (2) along A-Γ, the bands see considerably more dispersion due to the π–π stacking interactions between the aromatic linkers. It is, therefore, likely that the charge transport along the stacking direction will be preferred compared to within the layers, which is similar to what we observed previously for rare-earth–based HOTP materials.[13] Overall, the *ab initio* calculations agree with our hypothesis that charge transport in the material may happen preferentially along the π–π stacked columns of the linkers—explaining the similarities in electrical conductivities between **Ga_9(HOTP)$_4$** and its transition metal analogs.

Much of the attraction of electrically conductive MOFs lies in fine control over their structure and composition. Despite this, most works

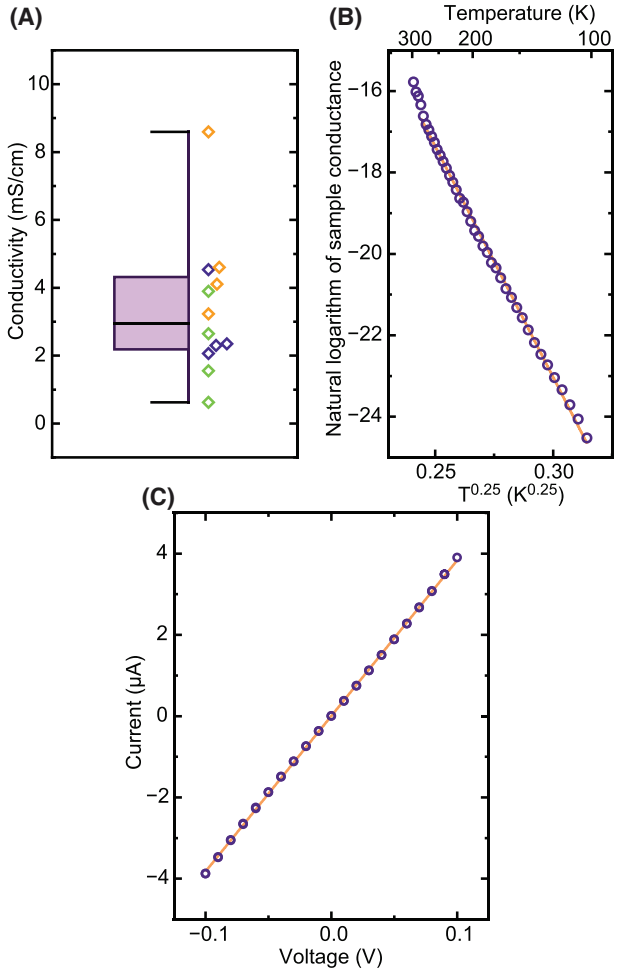

FIGURE 4 Electrical transport in $Ga_9(HOTP)_4$. (A) The material shows moderate electrical conductivities, with a median of 3.3 mS/cm. Colors of empty diamond markers denote different batches; the box and whisker plot depicts second and third quartiles, median (inner horizontal line), and minimum and maximum values (outer horizontal lines). Each data point represents a separate device. (B) The electrical conductivity is thermally deactivated (circles represent each data point) and is fit well by a 3D VRH model (solid orange line). (C) Sample I–V curve for a pressed pellet of the material, with circles representing a single data point, and the solid line shows the linear fit to the data ($R^2 = 0.999$) in accordance with Ohm's law.

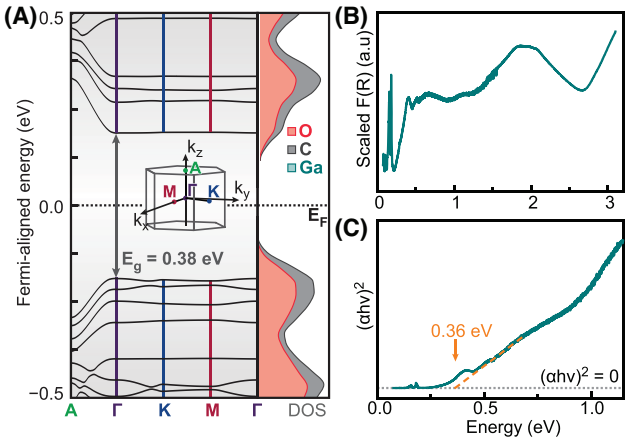

FIGURE 5 Electronic structure of $Ga_9(HOTP)_4$. (A) The electronic band structure of the material, obtained via density functional theory calculations, shows that the material is a narrow-gap semiconductor with a band gap of 0.38 eV. The bands along the A-Γ direction correspond to interactions along the *c* axis of the hexagonal direct cell and have considerably more spread than those along the Γ-K-M directions, which correspond to interactions within the *ab* plane. The density of states (DOS) diagram shows that the frontier bands are composed exclusively of the ligands' carbon- and oxygen-originated orbitals. Together, these two features show the importance of π–π stacking interactions in the material. (B) The diffuse reflectance spectrum of the material, presented as the Kubelka–Munk function F(R),[17] shows broadband absorption thereby giving an optical band gap of 0.36 eV via a Tauc plot[18] (C), matching the results of theoretical calculations.

on 2D layered conductive MOFs—the most conductive, and perhaps the most likely candidates for real-world applications—have so far been constrained in the variety of metal ions used mainly to first-row transition metals. In this work, we reported a new conductive MOF based on trivalent gallium, which had not been used in conductive MOFs. Through a combination of experimental and theoretical techniques, we have gained insight into the nature of electrical transport in this material and found π–π stacking interactions to be likely responsible for the conductivity. Although we have reached a similar conclusion previously with three-dimensional rare-earth–based conductive MOFs,[13] this work still provides useful new information due to the truly 2D nature of $Ga_9(HOTP)_4$. With the added benefit of an organic-solvent-less synthesis, we believe this work will both inspire a search for applications of the novel $Ga_9(HOTP)_4$ and inform the future design of conductive porous MOFs.

ACKNOWLEDGMENTS

The authors thank Dr. Lilia Xie for the helpful discussions. Work in the Dincă group was supported by the National Science Foundation (DMR-2105495). This material was also based upon work supported by the National Science Foundation through the Division of Materials Research under grant no. DMR-1956403 and the Cottrell Award.

COMPETING INTERESTS

The authors declare no competing interests.

AUTHOR CONTRIBUTIONS

G.S. and M.D. conceived and planned the study. G.S., C.H.H., and M.D. planned the experiments. C.H.H. and M.D. supervised the work. G.S. performed initial synthetic work and characterization and completed the structural investigation. G.C., with assistance from I.S., performed the final synthetic work and material characterization. K.N.L. performed the DFT calculations. G.S., G.C., and M.D. wrote the initial draft, which was revised and edited by all authors.

ORCID

Géraldine Chanteux https://orcid.org/0000-0001-5655-0536
Mircea Dincă https://orcid.org/0000-0002-1262-1264

PEER REVIEW

The peer review history for this article is available at: https://publons.com/publon/10.1111/nyas.14906.

REFERENCES

1. Xie, L. S., Skorupskii, G., & Dincă, M. (2020). Electrically conductive metal–organic frameworks. *Chemical Reviews*, *120*, 8536–8580.
2. Sheberla, D., Bachman, J. C., Elias, J. S., Sun, C.-J., Shao-Horn, Y., & Dincă, M. (2017). Conductive MOF electrodes for stable supercapacitors with high areal capacitance. *Nature Materials*, *16*, 220–224.
3. Miner, E. M., Wang, L., & Dincă, M. (2018). Modular O_2 electroreduction activity in triphenylene-based metal–organic frameworks. *Chemical Science*, *9*, 6286–6291.
4. Stassen, I., Dou, J.-H., Hendon, C., & Dincă, M. (2019). Chemiresistive sensing of ambient CO_2 by an autogenously hydrated Cu_3(hexaiminobenzene)$_2$ framework. *ACS Central Science*, *5*, 1425–1431.
5. Campbell, M. G., Sheberla, D., Liu, S. F., Swager, T. M., & Dincă, M. (2015). Cu_3(hexaiminotriphenylene)$_2$: An electrically conductive 2D metal-organic framework for chemiresistive sensing. *Angewandte Chemie*, *54*, 4349–4352.
6. Sheberla, D., Sun, L., Blood-Forsythe, M. A., Er, S., Wade, C. R., Brozek, C. K., Aspuru-Guzik, A. N., & Dincă, M. (2014). High electrical conductivity in Ni_3(2,3,6,7,10,11-hexaiminotriphenylene)$_2$, a semiconducting metal–organic graphene analogue. *Journal of the American Chemical Society*, *136*, 8859–8862.
7. Day, R. W., Bediako, D. K., Rezaee, M., Parent, L. R., Skorupskii, G., Arguilla, M. Q., Hendon, C. H., Stassen, I., Gianneschi, N. C., Kim, P., & Dincă, M. (2019). Single crystals of electrically conductive two-dimensional metal-organic frameworks: Structural and electrical transport properties. *ACS Central Science*, *5*, 1959–1964.
8. Bi, S., Banda, H., Chen, M., Niu, L., Chen, M., Wu, T., Wang, J., Wang, R., Feng, J., Chen, T., Dincă, M., Kornyshev, A. A., & Feng, G. (2020). Molecular understanding of charge storage and charging dynamics in supercapacitors with MOF electrodes and ionic liquid electrolytes. *Nature Materials*, *19*, 552–558.
9. Cui, J., & Xu, Z. (2014). An electroactive porous network from covalent metal–dithiolene links. *Chemical Communications*, *50*, 3986–3988.
10. Kambe, T., Sakamoto, R., Hoshiko, K., Takada, K., Miyachi, M., Ryu, J.-H., Sasaki, S., Kim, J., Nakazato, K., Takata, M., & Nishihara, H. (2013). π-Conjugated nickel bis(dithiolene) complex nanosheet. *Journal of the American Chemical Society*, *135*, 2462–2465.
11. Hmadeh, M., Lu, Z., Liu, Z., Gándara, F., Furukawa, H., Wan, S., Augustyn, V., Chang, R., Liao, L., Zhou, F., Perre, E., Ozolins, V., Suenaga, K., Duan, X., Dunn, B., Yamamto, Y., Terasaki, O., & Yaghi, O. M. (2012). New porous crystals of extended metal-catecholates. *Chemistry of Materials*, *24*, 3511–3513.
12. Rietveld, H. M. (1969). A profile refinement method for nuclear and magnetic structures. *Journal of Applied Crystallography*, *2*, 65–71.
13. Skorupskii, G., Trump, B. A., Kasel, T. W., Brown, C. M., Hendon, C. H., & Dincă, M. (2020). Efficient and tunable one-dimensional charge transport in layered lanthanide metal–organic frameworks. *Nature Chemistry*, *12*, 131–136.
14. Brunauer, S., Emmett, P. H., & Teller, E. (1938). Adsorption of gases in multimolecular layers. *Journal of the American Chemical Society*, *60*, 309–319.
15. Willems, T. F., Rycroft, C. H., Kazi, M., Meza, J. C., & Haranczyk, M. (2012). Algorithms and tools for high-throughput geometry-based analysis of crystalline porous materials. *Microporous and Mesoporous Materials*, *149*, 134–141.
16. Mott, N. F. (1969). Conduction in non-crystalline materials. *Philosophical Magazine*, *19*, 835–852.
17. Kubelka, P., & Munk, F. (1931). An article on optics of paint layers. *Zeitschrift für Physik*, *12*, 593–601.
18. Tauc, J. (1968). Optical properties and electronic structure of amorphous Ge and Si. *Materials Research Bulletin*, *3*, 37–46.

SUPPORTING INFORMATION

Additional supporting information can be found online in the Supporting Information section at the end of this article.

How to cite this article: Skorupskii, G., Chanteux, G., Le, K. N., Stassen, I., Hendon, C. H., & Dincă, M. (2022). Electrical conductivity through π–π stacking in a two-dimensional porous gallium catecholate metal–organic framework. *Ann NY Acad Sci.*, 1–5. https://doi.org/10.1111/nyas.14906